



**HAL**  
open science

## Structural Insights on Nitrogen-Containing Hydrothermal Carbon Using Solid-State MAS $^{13}\text{C}$ and $^{15}\text{N}$ NMR

Niki Baccile, Guillaume Laurent, Cristina Coelho, Florence Babonneau, Li Zhao, Maria-Magdalena Titirici

► **To cite this version:**

Niki Baccile, Guillaume Laurent, Cristina Coelho, Florence Babonneau, Li Zhao, et al.. Structural Insights on Nitrogen-Containing Hydrothermal Carbon Using Solid-State MAS  $^{13}\text{C}$  and  $^{15}\text{N}$  NMR. Journal of Physical Chemistry C, 2011, 115 (18), pp.8976-8982. 10.1021/jp2015512 . hal-01455162

**HAL Id: hal-01455162**

**<https://hal.sorbonne-universite.fr/hal-01455162>**

Submitted on 3 Feb 2017

**HAL** is a multi-disciplinary open access archive for the deposit and dissemination of scientific research documents, whether they are published or not. The documents may come from teaching and research institutions in France or abroad, or from public or private research centers.

L'archive ouverte pluridisciplinaire **HAL**, est destinée au dépôt et à la diffusion de documents scientifiques de niveau recherche, publiés ou non, émanant des établissements d'enseignement et de recherche français ou étrangers, des laboratoires publics ou privés.

**IMPORTANT NOTE: Please be aware that slight modifications occurring after Proof correction may occur between this version of the manuscript and the version on the Publisher's website**-----

# Structural Insights on Nitrogen-containing *Hydrothermal Carbon* using Solid-State MAS $^{13}\text{C}$ and $^{15}\text{N}$ NMR

*Niki Baccile*<sup>1\*</sup>, *Guillaume Laurent*<sup>1</sup>, *Cristina Coelho*<sup>1</sup>, *Florence Babonneau*<sup>1</sup>, *Li Zhao*<sup>2</sup>, *Maria-Magdalena Titirici*<sup>2</sup>

1-UPMC Univ Paris 06 and CNRS, UMR 7574, Chimie de la Matière Condensée de Paris, F-75005, Paris, France

2-Max-Planck Institute for Colloids, Research Campus Golm, D-14424 Potsdam, Germany

**RECEIVED DATE (to be automatically inserted after your manuscript is accepted if required according to the journal that you are submitting your paper to)**

CORRESPONDING AUTHOR FOOTNOTE

\* Corresponding Author. E-mail: niki.baccile@upmc.fr, Fax: +33 1 44 27 15 04

+ UPMC Univ Paris 06, Laboratoire de Chimie de la Matière Condensée de Paris, Collège de France, 11 place M. Berthelot, F-75005, Paris, France

**ABSTRACT**

Here,  $^{13}\text{C}$  and  $^{15}\text{N}$  solid state NMR is used as the main and most effective characterization technique on nitrogen-containing hydrothermal carbons obtained from glucose and glycine. This study

represents a model system for other types of nitrogen-containing hydrothermal carbons, which were shown to have interesting energy-storage properties (Zhao *et al. Adv. Mater.*, **2010**, *22*, 5202). These materials are obtained either from N-containing carbohydrates or from pure carbohydrates in the presence of natural amino-containing compounds such as proteins or aminoacids. In contrast to what is generally known for this model system, high molecular weight heterogeneous polymers that are formed when sugars and amino acids combine through the Maillard reaction (e.g., melanoidins), we found an extended nitrogen-containing aromatic network which is chemically bound to a polyfuran network known to be one of the main components of the biomass derived hydrothermal carbons. In contrast to the hydrothermal carbons obtained from pure carbohydrates, these types of N-containing materials have an increased level of aromatic character already present at 180°C, after the hydrothermal treatment.

**KEYWORDS.** Nitrogen Doped Carbons, Hydrothermal Carbonization, Glucose, Glycine, <sup>13</sup>C solid-state MAS NMR, Double quantum NMR, sugar-amino acids interactions.

## **Introduction**

In the past 10 years, the hydrothermal treatment of biomass has gained an increasing interest in the field of material science. Many studies focus already on both applications<sup>1</sup> and fundamental<sup>2</sup> aspects motivated by the interest in producing carbonaceous powders with tunable sizes and surface properties directly from raw, processed and even waste biomass<sup>3</sup>. Recent review articles can be consulted for an overview on the progress regarding this topic over the past few years<sup>4</sup>. The most interesting point of this approach is undoubtedly the perspective of processing waste biomass (lignins, cellulose, starch) into valuable carbonaceous materials although the main research so far has been done using pure carbohydrates normally present in biomass composition. One of the main reasons for that is the fact that the chemical reactions which transform saccharides into hydrothermal carbons are extremely complex and they had first to be understood starting from

simple model systems<sup>5</sup>. It is widely known that saccharides dehydratize to form furans<sup>6</sup> and we have already pointed out the importance of such intermediate reactants in the formation of the final material. Different techniques like FT-IR<sup>2b</sup>, XPS and XRD<sup>7</sup> have been used to identify the structure of the amorphous material but, so far, the best results regarding the final structure of such carbon materials were obtained by using advanced solid state NMR techniques<sup>2a</sup>, which attested the presence of an abundant polyfuran core instead of the expected aromatic network, previously reported by other authors<sup>2b</sup>.

One important advantage of these carbons is undoubtedly the possibility of modifying the surface<sup>8</sup> or the bulk of the carbonaceous network by introducing hetero atoms such as transition metals<sup>1i, 1q, 9</sup> or nitrogen<sup>10</sup>. Hybrid metal-carbon nanostructures have been obtained with potential application in catalysis. The introduction of N-atoms within the bulk or at surface structure of these materials is extremely interesting given the multitude of applications such as, for example, pH-responsive adsorbents<sup>11</sup>, supercapacitors<sup>12</sup>, fuel cell electrodes<sup>13</sup>, CO<sub>2</sub> adsorbers<sup>14</sup> and materials with extremely high conductivities<sup>15</sup>. We have recently shown the possibility of making nitrogen-rich carbon nanoparticles using a mixture of glucose and ovalbumin<sup>16</sup>, while glucosamine and chitosan<sup>10</sup> can also be used as simultaneous nitrogen sources. Preliminary results show a very good and highly selective CO<sub>2</sub> uptake suggesting that such materials could be successful candidates as CO<sub>2</sub> sequestration agents<sup>17</sup> or for use in supercapacitors<sup>18</sup>. For this reason we want to address the problem of structural identification no matter which natural nitrogen sources, like aminosugars, aminoacids or proteins, are used. We will use both <sup>13</sup>C and <sup>15</sup>N solid state NMR experiments to identify carbon and nitrogen sites and compare the structure of a nitrogen-containing material to a nitrogen-free one, pointing out the most important structural differences. In particular, a double isotope-enriched glucose-glycine mixture will be used as model system and compared to non-enrichable ones. In addition, we will show that the hydrothermal treatment of glucose and glycine, which is the classical reaction to make melanoidin resins, actually leads to a highly complex material with an unexpected structure of very different nature than typical melanoidin resins

themselves, which were recently investigated by a combination of advanced  $^{13}\text{C}$  and  $^{15}\text{N}$  solid state NMR experiments<sup>19</sup>.

Here, we will use a multinuclear NMR approach to show that the combination of longer reaction times and higher temperatures under hydrothermal conditions drastically brings the widely known Maillard reaction between glucose and glycine to its extreme condensation products characterized with a high load of aromatic nitrogen-containing groups, which were not observed before in the final raw material. Interestingly, no matter the complexity of the nitrogen source, the final material seems to have very close structural features. The better knowledge of the nitrogen-containing carbonaceous structure should help understanding the energy-storage properties of these materials and, eventually, improve and control them through synthesis.

### **Experimental Section**

**Sample *HC gly-C13-N15-gly* preparation.** 10 mL of a deionized water solution containing 1g of fully labeled D-Glucose- $^{13}\text{C}_6$  (Aldrich, CAS:110187-42-3) and 0.4 g of glycine- $^{15}\text{N}$  (Aldrich, CAS: 7299-33-4) is inserted into a glass vial inside a typical PTFE-lined autoclave system for hydrothermal reaction at 180°C for 24h. After reaction, the autoclave is cooled down in a water bath at room temperature. The obtained black solid powder is then separated from the remaining aqueous solution by centrifugation (7000 rpm for 20 minutes) and dried at 80°C in an oven under vacuum during 12 hours.

Scanning Electron Microscopy (SEM) images were acquired on a LEO 1550/LEO GmbH Oberkochen provided with an Everhard Thornley secondary electron and In-lens detectors. Elemental analysis. Chemical analysis was performed on a (C, N, O, S, H) Elementar Vario Micro Cube.

NMR experiments.  $^1\text{H}$  and  $^{13}\text{C}$  solid-state Magic Angle Spinning (MAS) NMR experiments have been acquired on a Bruker Avance 300 MHz (7 T) spectrometer using 4 mm zirconia rotors spinning at a MAS frequency of  $\nu_{\text{MAS}} = 14$  kHz.  $^1\text{H}$  and  $^{13}\text{C}$  chemical shifts were referenced relative to tetramethylsilane (TMS;  $\delta = 0$  ppm). Details on one pulse MAS, Cross Polarization (CP) MAS,

Inversion Recovery Cross Polarization (IRCP), CP MAS homonuclear single-quantum double-quantum (SQ-DQ)  $^{13}\text{C}$  correlation experiments have been published elsewhere<sup>2a</sup>.

$^{15}\text{N}$  one pulse experiments were performed on a Bruker Avance 500 MHz (11.7 T) spectrometer using 7 mm zirconia rotors at  $\nu_{\text{MAS}} = 5$  kHz. An anti-ring pulse programme (ARING) with a  $90^\circ$  pulse angle of  $7.70 \mu\text{s}$  was used. Recycle delay of 30 s and number of transients of 2000 were found to be optimal conditions.  $^{15}\text{N}\{^1\text{H}\}$  CP-MAS experiments were done using a recycle delay of 3 s and a contact time of 2 ms, TPPM decoupling was applied during signal acquisition and the number of transients was 7200.

Triple resonance CPMAS  $^{13}\text{C}\{^1\text{H},^{15}\text{N}\}$  heteronuclear correlation was recorded on a 700 MHz (16.4 T) spectrometer with a 3.2 mm zirconia rotor ( $\nu_{\text{MAS}} = 22$  kHz) using a triple  $^1\text{H}$ -X-Y probe. A standard double CP pulse scheme (Sup Mat Figure1) was used. Typical acquisition values were: proton  $90^\circ$  flip angle,  $t^{90^\circ} = 2.75 \mu\text{s}$ ,  $^{15}\text{N}\{^1\text{H}\}$  and  $^{13}\text{C}\{^{15}\text{N}\}$  contact times,  $t_{c1} = 5$  ms and  $t_{c2} = 1$  ms, 64 increments in the indirect dimension, and 1200 transients. Quadrature detection was achieved using the States method<sup>20</sup>.

## Results

As pointed out already in the introduction, given the amorphous nature of HC and their chemical heterogeneity, it is impossible to perform a clear-cut structural study using characterization techniques like XRD, infrared spectroscopy or even XPS, whose poor resolution does not provide full pieces of information. Recently, we have used solid state NMR to solve the structure of hydrothermal carbon from glucose<sup>2a</sup> and identify nitrogen sites in glucosamine-derived HC samples<sup>10</sup>. Similar experiments are very helpful whenever chemical enrichment is possible, which is seldom the case, especially if raw biomass is employed in the synthesis of HC. For this reason, we concentrated our attention onto the glycine-glucose derived HC as a model system. We employed  $^{15}\text{N}$ -glycine and  $^{13}\text{C}$ -glucose both as spin-1/2 nitrogen and carbon sources.

Some preliminary morphological studies of nitrogen-doped hydrothermal carbon powders obtained from glucose and glycine are very similar to the previously synthesized carbon materials<sup>5,2a</sup>. Sup Mat Figure 2 shows SEM micrographs of typical spherical microparticles as usually obtained from the hydrothermal carbonization process. The elemental composition shows that about  $8.4 \pm 0.5$  w% of nitrogen is incorporated inside the material (C:  $63.3 \pm 1.0$  w%, H:  $5.5 \pm 1.0$  w%); this value is comparable with the ones obtained in the presence of the ovalbumin protein<sup>16</sup> as well as from glucosamine<sup>10</sup>. Even if elemental analysis shows that nitrogen is successfully incorporated in the sample, nothing can be told about the nature of the N sites and whether the glycine motif is kept intact as in the case of melanoidins<sup>19</sup> or underwent chemical modification. <sup>13</sup>C and <sup>15</sup>N solid state NMR experiments discussed below will bring a detailed answer to these questions.

The first point to be addressed is the validity of using the glucose-glycine mixture as model compound. Figure 1 shows the <sup>13</sup>C CP MAS response of a set of nitrogen-containing samples obtained from the hydrothermal treatment of and glucose/albumin<sup>16</sup>, <sup>15</sup>N-glucosamine<sup>10</sup> (Figure 1c) the mixtures <sup>13</sup>C-glucose/<sup>15</sup>N-glycine (Figure 1d) compared with pure glucose (Figure 1a) . We have previously observed<sup>2a</sup> that a contact time of 3 ms is enough to homogeneously excite the whole <sup>13</sup>C population, allowing a qualitative but reliable comparison among the relative intensities of the <sup>13</sup>C resonance peaks. A close comparison among the spectra shows very similar features: the amount of C=O groups (200-210 and 175 ppm) and aliphatic carbons (10-60 ppm) is significant unless glucosamine alone is used; the aromatic region is dominated by a large intense peak between 123 and 130 ppm (shaded region in Figure 1), which is generally absent when glucose (Figure 1a) alone is processed, and two peaks at 150 and 110 ppm, assigned to, respectively, C=C-O and HC=C-O groups. The resonance in the aromatic region around 125 ppm is very intense for the *HC glu-C13-N15-gly* system, indicating a larger aromatic network, whose existence is hard to prove in the *HC glu* sample. In fact, we have previously<sup>2</sup> shown that hydrothermal treatment of glucose provides a carbonaceous scaffold whose amorphous structure is dominated by an extended furan-

type network. For this reason and given the possibility to use  $^{13}\text{C}$ -enriched glucose and  $^{15}\text{N}$ -enriched glycine, we show hereafter a full structural study of their hydrothermal derivative with our discussion based on the C-H, C-N and C-C local environments.

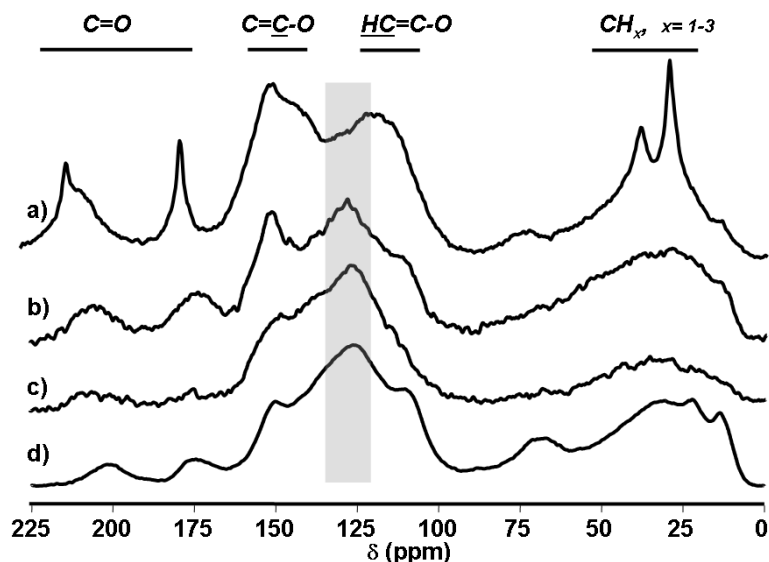


**Figure 1 –  $^{13}\text{C}$  CP MAS NMR experiments ( $t_c = 3$  ms) recorded on pure  $^{13}\text{C}$ -glucose-derived carbons (HC glu) and several nitrogen-containing hydrothermal carbon materials: (a) sample HC glu; (b) HC glu-albumin; (c) HC glu- $^{15}\text{N}$ -glucosamine; (d) HC glu- $^{13}\text{C}$ - $^{15}\text{N}$ -gly. In (a) glucose is used alone but it can co-react with (b) ovalbumin<sup>16</sup> and (c)  $^{15}\text{N}$ -glucosamine.<sup>10</sup> In (d),  $^{13}\text{C}$ -glucose reacts in presence of  $^{15}\text{N}$ -glycine. Note: the better signal-to-noise ratio of HC glu and HC glu- $^{13}\text{C}$ - $^{15}\text{N}$ -gly derives from  $^{13}\text{C}$  enrichment.**

The structural investigation of the nitrogen-containing carbonaceous material is done according to a previously published experimental line.<sup>2a</sup> In that occasion, different NMR techniques were combined together to identify the main constituents of the carbonaceous scaffold obtained from hydrothermal treatment of glucose. Here, a similar approach is used; in particular, one-pulse  $^{13}\text{C}$  and  $^{15}\text{N}$  MAS NMR experiment allows the quantitative identification of all carbon and nitrogen sites and are presented here in Figure 2a and Figure 3a; cross polarization (CP) and inversion recovery cross polarization (IRCP) experiments give an unambiguous insight on protonated carbons and nitrogen sites; in particular, IRCP helps discriminating between CH, CH<sub>2</sub> and CH<sub>3</sub> groups<sup>21</sup>. Figure 2b and Figure 3b present  $^{13}\text{C}$  and  $^{15}\text{N}$  CP MAS experiments performed at a given contact time but the full set of data on CP and IRCP experiments can be found in Sup Mat Figure 3 and Sup Mat Figure 4. Finally, two-dimensional SQ-DQ  $^{13}\text{C}$  and HETCOR  $\{^1\text{H}\}^{15}\text{N}$ - $^{13}\text{C}$  experiments allow



identification of, respectively, carbon environments within one C-C atomic bond<sup>2a, 22</sup> and NH-C proximities.

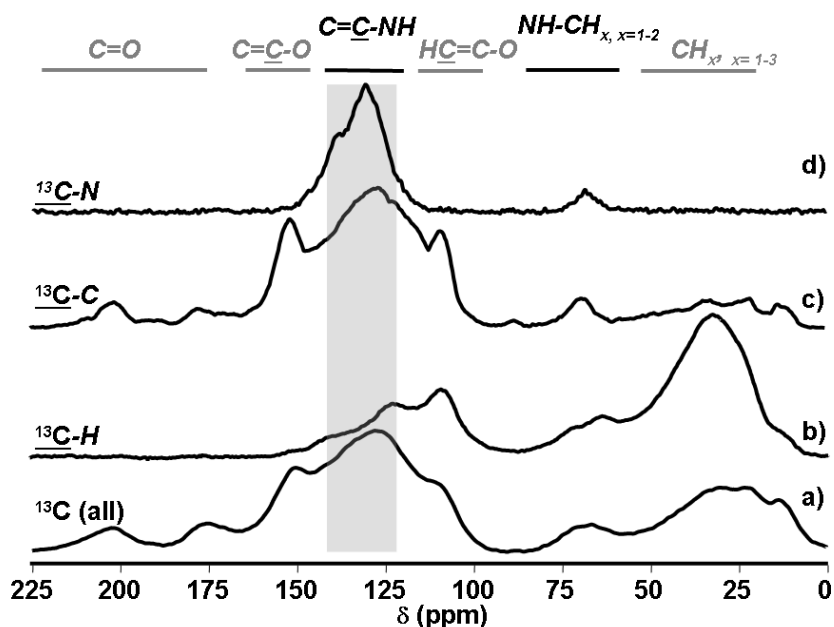


**Figure 2 - Comparison between  $^{13}\text{C}$  MAS NMR experiments acquired on the *HC glu-C13-N15-gly* system under the following conditions: a) one-pulse; b) CP performed at  $t_{\text{ct}} = 50 \mu\text{s}$ ; c) projection from the SQ-DQ  $^{13}\text{C}$  experiment at  $t_{\text{c}} = 3 \text{ ms}$ ; d) projection from the HETCOR  $^{15}\text{N}$ - $^{13}\text{C}$  experiment.**

### *Carbon-proton proximities*

Chemical shift analysis combined with cross-polarization experiments were used to discriminate between carbonyl, aromatic and aliphatic groups (Figure 2b). In particular, variation of contact time in CP experiments (Sup Mat Figure 3c) nicely allows to discriminate between protonated and non protonated  $\text{sp}_2$  carbons while IRCP experiments give an insight on the degree of protonation of aliphatic carbon atoms (Sup Mat Figure 3 a,b).

### *Carbon-nitrogen proximities*

The structural analysis was completed by one-pulse nitrogen-15 and  $^{15}\text{N}\{^1\text{H}\}$  cross polarization NMR experiments (Figure 3). First of all, in good agreement with elemental analysis ( $8.4 \pm 0.5 \text{ w\%}$ ) these experiments clearly show that nitrogen is well introduced inside the carbonaceous network and it is surrounded by different carbon environments. Chemical shifts at -75 and -250 ppm

indicate, respectively, sp<sup>2</sup> and sp<sup>3</sup> nitrogen-carbon bonds.  $\{^1\text{H}\}^{15}\text{N}$  CP (Figure 3b) only shows protonated nitrogen sites, whose chemical shift range (-200/-300 ppm) indicates the presence of amide or pyrrole groups<sup>23</sup>; interestingly, amine groups which are initially introduced via the glycine molecule, have massively reacted since the NH<sub>2</sub> resonance at -330 ppm is very low; additionally, the  $^{15}\text{N}$  one pulse experiment (Figure 3a) shows non-protonated aromatic, pyridinic and pyrazine-like groups (0-150 ppm).

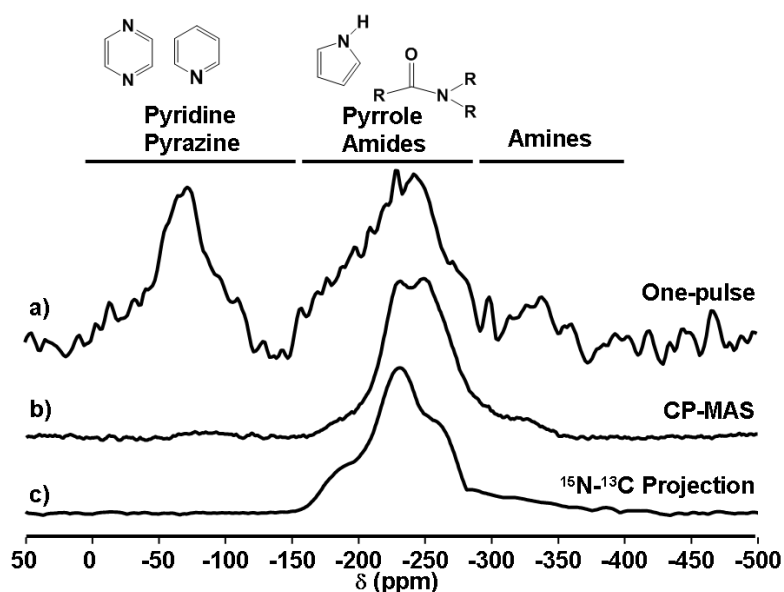


Figure 3 –  $^{15}\text{N}$  one-pulse and CP-MAS (with 2 ms contact time) spectra of *HC glu-C13-N15-gly* and  $^{15}\text{N}$  projection of the  $^{13}\text{C}\{^1\text{H}, ^{15}\text{N}\}$  HETCOR experiment.

This preliminary analysis shows very interesting features which make this material very different from the hydrothermal carbon obtained from pure glucose<sup>2a</sup>; in particular, the introduction of nitrogen induces a systematic aromatization of the carbonaceous network.

Deeper insights on the type of C-C and N-C bonds can be obtained from the  $^{13}\text{C}\{^1\text{H}, ^{15}\text{N}\}$  triple resonance cross polarization NMR experiments shown in Figure 4. Here, an initial  $^{15}\text{N}\{^1\text{H}\}$  cross polarization step at an optimum contact time ( $t_{c1} = 5$  ms) excites all protonated nitrogen atoms (Figure 3); then, polarization is transferred to  $^{13}\text{C}$  nuclei via a second contact time ( $t_{c2} = 1$  ms) which was chosen long enough to detect a signal with a reasonable signal-to-noise ratio but short enough to probe the shortest possible C-N distances. The use of the proton bath to excite the  $^{15}\text{N}$

spins limits the accessibility to solely N-H groups (-150/-300 ppm) with respect to the entire nitrogen population which also includes aromatic sites (0/-150 ppm) (Figure 3a). Any attempt to run a complementary  $^{15}\text{N}\{^1\text{H}, ^{13}\text{C}\}$  experiment failed. For this reason, we stress the fact that the results obtained from this experiment only concern protonated nitrogen environments.

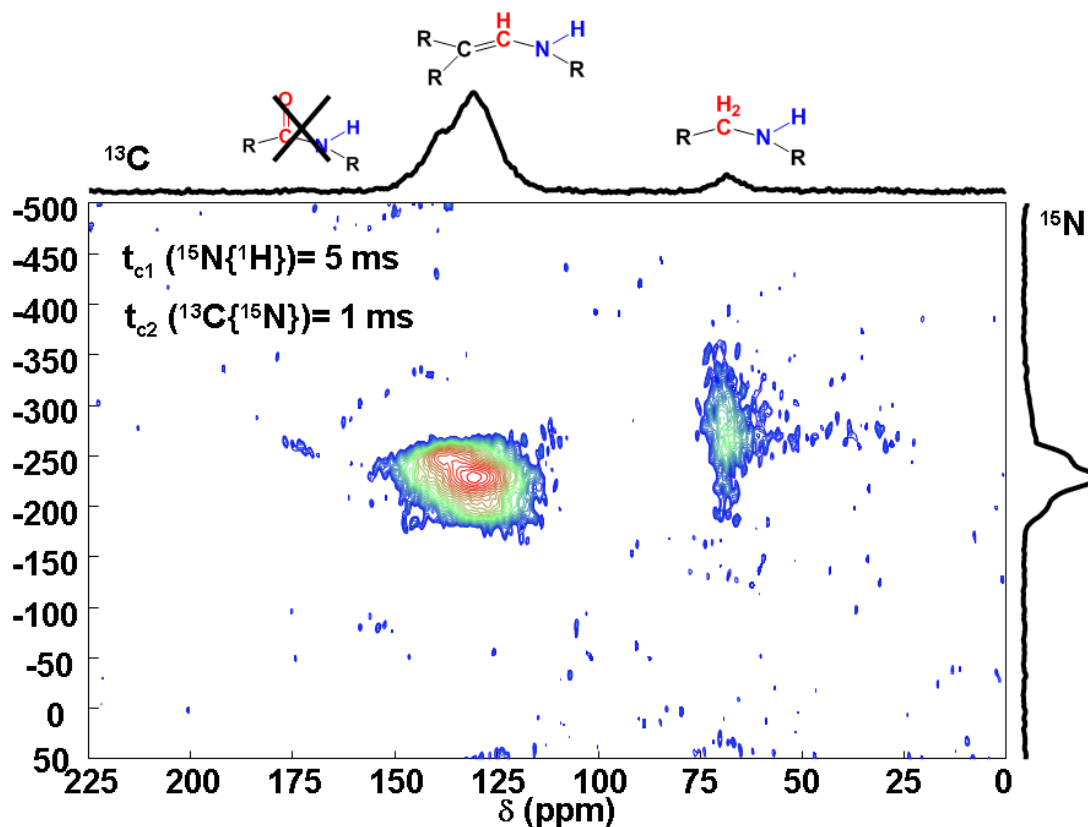


Figure 4 – 2D map showing the double CP  $^{13}\text{C}\{^1\text{H}, ^{15}\text{N}\}$  experiment on the *HC glu--C13-N15-gly* system and obtained with pulse sequence shown in Sup Mat Figure 1. Contact times for each cross polarization step are given in the figure. Insight on the possible chemical groups are reported in Figure 5. Note that here “R” is just a general notation to refer to C or H elements.

The 2D  $^{13}\text{C}\{^1\text{H}, ^{15}\text{N}\}$  map in Figure 4 provides a direct fingerprint of the nitrogen-to-carbon proximities. The  $^{15}\text{N}$ -filtered  $^{13}\text{C}$  projection shows two main regions, one with two peaks at 130.0 and 136.7 ppm and the other at 70 ppm while the  $^{15}\text{N}$  projection shows three resonances at about -195.0, -230.0 and -250.0 ppm. As expected, these values are comparable with simple  $^{15}\text{N}\{^1\text{H}\}$  CP experiments in Figure 3. A deep look at the 2D map shows that C=CH-NH groups are the most abundant species in the material, followed by  $\text{CH}_x\text{-NH}$  species. On the contrary, no specific correlation is found between (protonated) nitrogen and carbonyl groups, suggesting that amides are

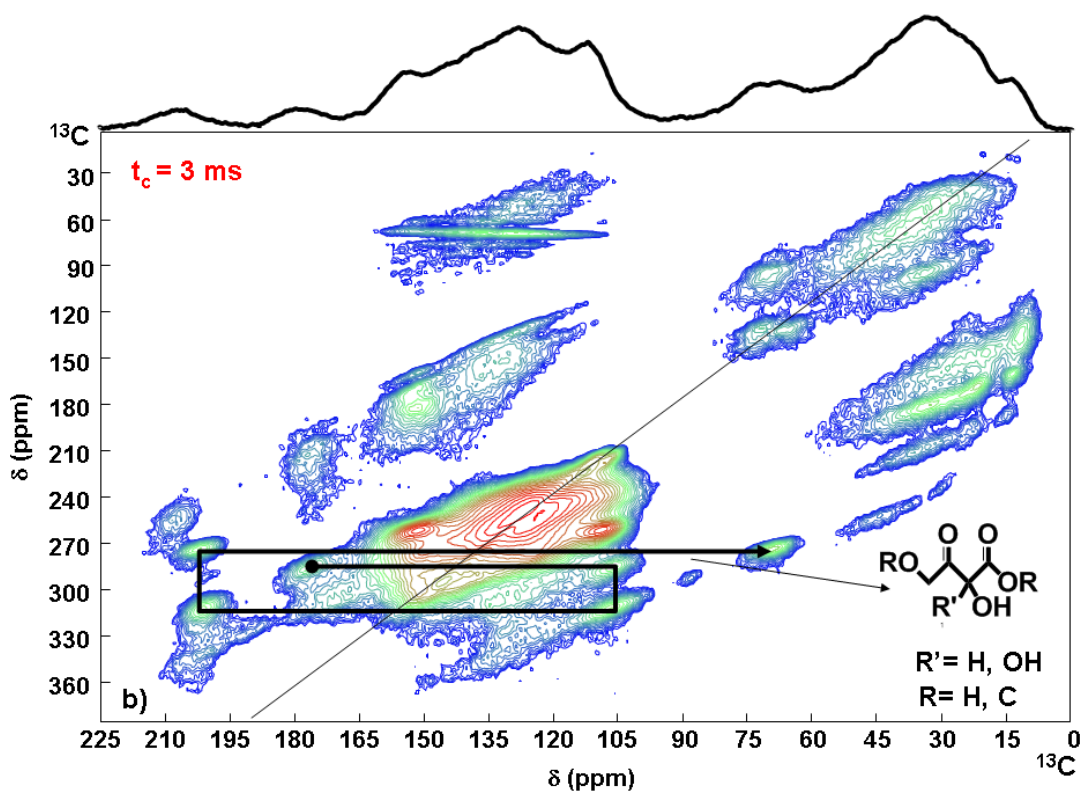
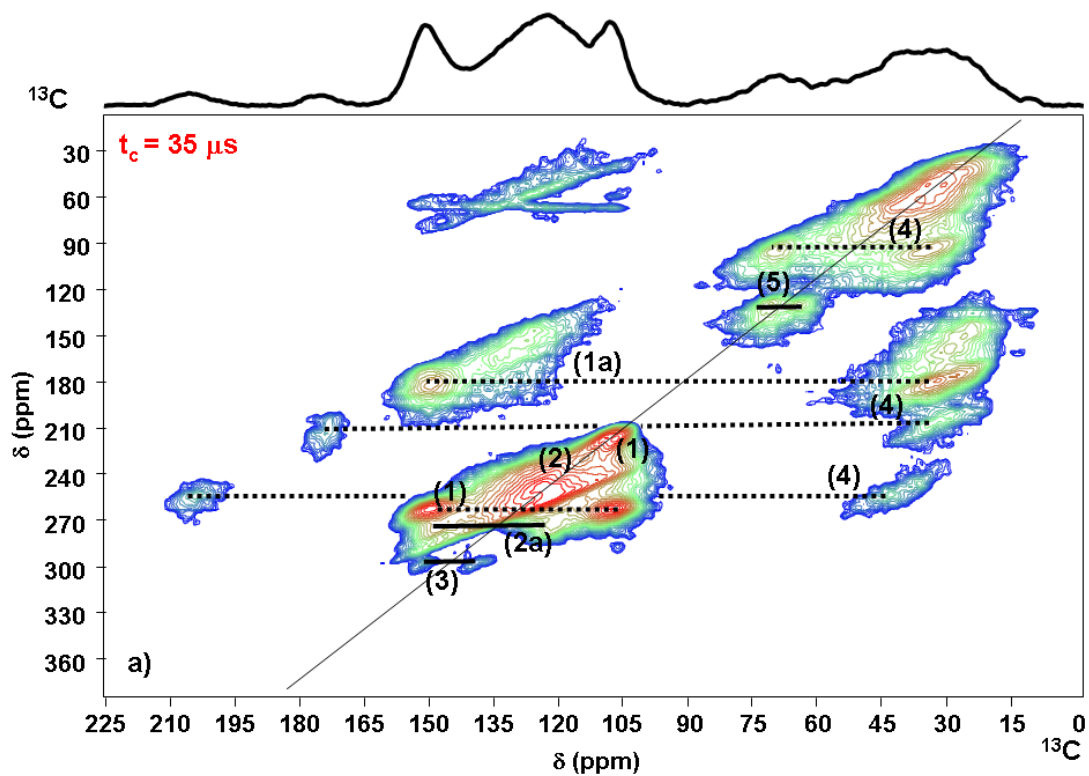
not relevant. This result is quite interesting as it suggests that the signal between 130.0 and 136.0 ppm mainly relates to pyrolic species.

#### *Carbon-carbon connectivities*

Two double quantum single quantum correlation experiments were recorded in order to select different types of carbon environments. In the first one (Figure 5a), a  $^{13}\text{C}\{^1\text{H}\}$  contact time ( $t_c$ ) of 35  $\mu\text{s}$  was employed before the excitation of DQ  $^{13}\text{C}$  coherences while in the second one (Figure 5b) the  $t_c$  was much longer (3 ms). The shorter the  $t_c$ , the higher the selectivity to detect protonated carbons. In both cases the SQ-DQ  $^{13}\text{C}$  excitation and reconversion time was the same (285.7  $\mu\text{s}$ ) and chosen in order to observe only the direct carbon-carbon bonds<sup>2a,22</sup>.

At short contact time (35  $\mu\text{s}$  - Figure 5a), most of the constitutive chemical units can be identified. In particular, (1) and (1a) refer to the classical furane unit connected to aliphatic groups via the  $\alpha$ -carbon atom while (4) shows keto-aliphatic and intra-aliphatic bonds. These species were already observed on the glucose-derived hydrothermal carbon and are quite typical for these materials<sup>2a</sup>. Additionally, more specific bonds can be identified in this nitrogen-containing sample. First of all, the on-diagonal cross-peak at 127.5 ppm (2) now dominates the 2D map (Figure 5a,b); in particular, its on-diagonal position suggests the existence of abundant aromatic units while the off-diagonal (2a) peaks at  $\delta = 151$  and 109 ppm suggest the presence of possible phenols. The cross-peak at 127.5 ppm also indicates the existence of possible pyrazine or pyridine units that can be related to the existence of the broad peak at -75 ppm in the one-pulse  $^{15}\text{N}$  spectrum in Figure 3. Finally, specific furanic-aromatic bonds could also be proposed (2a). Pyrrole-type compounds, proposed after the  $^{13}\text{C}\{^1\text{H}, ^{15}\text{N}\}$  HETCOR experiment, could be justified by cross-peaks (3) while NH-CH groups should be observed in (5). At longer contact times, the SQ-DQ experiment does not bring further information on the material core-network but it shows the existence of newly appearing and self-correlating cross-peaks, as outlined by the connecting black arrow. In particular,

the COOH group at 176 ppm is readily connected to a cheto-bond (202 ppm) through a chemical group resonating at 106 ppm, whose exact attribution constitutes a harsh task at the moment. These



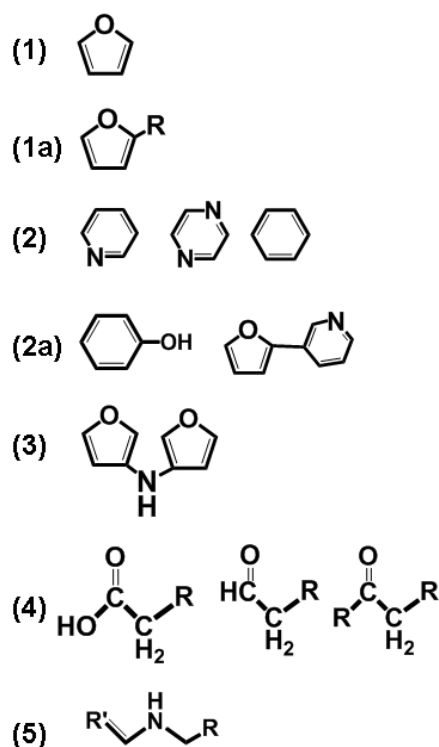


**Figure 5 – *HC glu-C13-N15-gly*. SQ-DQ  $^{13}\text{C}$  maps obtained for equal double quantum excitation and reconversion times (285.7  $\mu\text{s}$ ). Contact time before double quantum coherences excitation is  $t_c = 35 \mu\text{s}$  (a) and  $t_c = 3 \text{ ms}$  (b).**

cross-peaks probably identify isolated or grafted molecules whose lack of signal at short contact times rather depends on their mobility (less efficient cross polarization transfer) than on the lack of protonated environment; in fact, CP and IRCP experiments show that carbon peaks at 70.6 ppm and 106.7 ppm are indeed protonated. In Figure 5b we propose the possible molecular structure, which, according to the exact nature of R and R' groups, may be related to organic acids-derivatives (e.g., dihydroxyfumaric acid, tartaric acid or dehydroascorbic acid).

After combining the pieces of information obtained from one-pulse, CP, IRCP, HETCOR  $^{15}\text{N}$ - $^{13}\text{C}$  and SQ-DQ  $^{13}\text{C}$  experiments presented above, the deconvolution of the one-pulse  $^{13}\text{C}$  spectrum (Sup Mat Figure 4) of the *HC glu- $^{13}\text{C}$ - $^{15}\text{N}$ -gly* sample (Figure 2a) shows not less than 25 different carbon species, whose list of resonances, chemical shift values and tentative attribution is listed in Supp Mat Table 1.

If compared with literature, the glucose/glycine system is well-known for its reactivity in hydrolytic medium undergoing Maillard reaction, which is at the origin of the non-enzymatic

browning in food chemistry and in the synthesis of melanoidin resins<sup>19,24</sup>. Nevertheless, the conditions employed in the HC process higher temperatures (temperatures above 160°C, self-generated pressures - 10-30 bars – and residence times between 12 and 24 hours) produce a different material: typical melanoidins keep up to 60% of glycine molecules intact and formation of pyrazines and pyridines is generally not observed while <sup>13</sup>C and <sup>15</sup>N NMR experiments on glycine-derived HC's show no trace of leftover glycine and the overall amount of NH<sub>2</sub> groups has almost quantitatively reacted further. Maillard reaction cascades are the most probable pathways that transform sugar, sugar derivatives and amines into cyclic compounds but the formation of modified pyrazines<sup>25</sup>, furanones, pyranones<sup>26</sup> and pyrroles<sup>24b</sup> is largely documented more as degradation compounds rather than as network-forming bricks.

To go further, one should not forget that the main degradation product of glucose is hydroxymethylfurfural (HMF), which is the main reactive compound in the formation of hydrothermal carbon<sup>2a,5</sup> and that spectroscopic signature of furane rings is still abundant in the final nitrogen-containing HC material. The C site in  $\alpha$ -position in furan rings and their derivatives can easily polymerize via radical, cationic or anionic reactions<sup>27</sup>; nitrogen-containing derivatives of HMF can also be synthesised as precursors for linear and branched polymers<sup>28</sup> but the chemical processes behind are still quite unclear because the reaction between glucose, furans and glycine does not stop at the simple glycine incorporation and methods to follow the reactions in-situ are at the moment not developed yet.

## **Conclusions**

Nitrogen-containing carbons constitute a new class of interesting energy-storage materials. The use of renewable resources in combination of hydrothermal treatment also constitutes a cheap way to introduce nitrogen within a carbonaceous scaffold. Nevertheless, the complexity of the reaction mechanism and of the final structure itself constitute a barrier to the understanding, though the improving, of these materials.

Treating natural nitrogen-containing molecules such as aminoacids or proteins with glucose or aminated saccharides such as chitosan or glucosamine under hydrothermal conditions provide the formation of nitrogenated materials up to 8-10 w%. Here, we have carried out a specific structural study on the glycine/glucose system using solid state NMR and isotopically-enriched ( $^{13}\text{C}$  and  $^{15}\text{N}$ ) sources. One-dimensional  $^{13}\text{C}$  experiments (one-pulse and CP MAS) showed that all hydrothermal carbons have very similar structures no matter the complexity of the carbon source. Then, the presence of extended aromatic domains in coexistence with the expected furan network is documented and constituted the main feature of these materials.

Finally, the combination of one-dimensional (CP, IRCP) and two-dimensional (single quantum double quantum  $^{13}\text{C}$ , double CP  $^{13}\text{C}\{^1\text{H}, ^{15}\text{N}\}$ ) experiments help drawing the carbon-to-carbon and carbon-to-nitrogen chemical arrangements. We were able to propose several possible structures which include the presence of pyrazine motifs connected to furans and we showed the quasi-absence of  $\text{NH}_2$  groups. Interestingly, the structure of such a material is very atypical for the Maillard reaction between glucose and glycine, which normally react to give melanoidin resins for which only the byproducts were shown to contain aromatic nitrogens but never the final solid. There is no trace left of the initial glycine and glucose. Instead they completely rearranged into an extended pyrazo-furanic matrix. The exact mechanism is still ambiguous but possible reactions between the alpha-carbons of furans and the pyrazines is a possible explanation.



## References

---

- <sup>1</sup> a) White, R. J. ; Budarin, V. L. ; Clark, J. H. *ChemSusChem*. **2008**, 1, 408-411.; b) Yao, C.; Shin, Y.; Wang, L. Q.; Windisch, C. F.; Samuels, W. D.; Arey, B. W.; Wang, C.; Risen, W. M.; Exarhos, G. J. *J. Phys. Chem. C* **2007**, 111, 15141-15145. c) Budarin, V. L.; Clark, J. H.; Luque, R.; Macquarrie, D. J.; Koutinas, A.; Webb, C. *Green Chem.* **2007**, 9, 992-995. d) Budarin, V.; Luque, R.; Macquarrie, D. J.; Clark, J. H. *Chem.-Eur. J.* **2007**, 13, 6914-6919. e) Yu, S. H.; Cui, X. J.; Li, L. L.; Li, K.; Yu, B.; Antonietti, M.; Colfen, H. *Adv. Mater.* **2004**, 16, 1636 f) Tusi, M. M.; Brandalise, M.; Correa, O. V.; Oliveira Neto, A.; Linardi, M.; Spinacé, E. V. *Mater. Res.* **2007**, 10, 171-175. g) Sevilla, M.; Lota, G.; Fuertes, A. B. *J. Power Sources* **2007**, 171, 546-551. h) Qian, H. S.; Lin, G. F.; Zhang, Y. X.; Gunawan, P.; Xu, R. *Nanotechnology*, **2007**, 18. i) Cui, X. J.; Antonietti, M.; Yu, S. H. *Small*, **2006**, 2, 756-759. l) Sun, X. M.; Liu, J. F.; Li, Y. D.; *Chem.-Eur. J.* **2006**, 12, 2039-2047. m) Sun, X. M.; Li, Y. D. *Angew. Chem. Int. Ed.*, **2004**, 43, 597-601. n) Yang, H. X.; Qian, J. F.; Chen, Z. X.; Ai, X. P.; Cao, Y. L., *J. Phys. Chem. C.*, **2007**, 111, 14067-14071. o) Zhu, K.; Egeblad, K.; Christensen, C. H., *Eur. J. Inorg. Chem.*, **2007**, 3955-3960. p) Hu, J.; Li, H.; Huang, X. J., *Solid State Ion.*, **2007**, 178, 265-271. q) Titirici, M.-M.; Antonietti, M.; Thomas, A., *Chem. Mater.*, **2006**, 18, 3808-3812. r) Sun, X.; Li, Y. *Angew. Chem. Int. Ed.*, **2004**, 116, 3915-3919
- <sup>2</sup> a) Baccile, N.; Laurent, G.; Babonneau, F.; Fayon, F.; Titirici, M.-M.; Antonietti, M. *J. Phys. Chem. C*, **2009**, 113, 9644-9654; b) Sevilla, M.; Fuertes, A. B., *Chem. Europ. J.*, **2009**, 15, 4195 - 4203
- <sup>3</sup> White, R. J.; Antonietti, M.; Titirici, M.-M., *J. Mater. Chem.*, **2009**, 19, 8645-8650
- <sup>4</sup> a) Hu, B.; Yu, S.-H.; Wang, K.; Liu, L.; Xu, X.-W., *Dalton Trans.*, **2008**, 5414-5423; b) Titirici, M.-M.; Antonietti, M., *Chem. Soc. Rev.*, **2010**, 39, 103-116; c) Hu, B.; Wang, K.; Wu, L.; Yu, S.-H.; Antonietti, M.; Titirici, M.-M., *Adv. Mater.*, **2010**, 22, 1-16
- <sup>5</sup> Titirici, M.-M.; Antonietti, M.; Baccile, N., *Green Chem.*, **2008**, 10, 1204-1212
- <sup>6</sup> a) Lourvanij, K.; Rorrer, G. L., *Appl. Catal. A*, **1994**, 109, 147; b) Lourvanij, K.; Rorrer, G. L., *Ind. Eng. Chem. Res.*, **1993**, 32, 11; c) Antal, M. J.; Mok, W. S. L.; Richards, G. N., *Carbohydr. Res.*, **1990**, 199, 91
- <sup>7</sup> Titirici, M.-M.; Thomas, A.; Antonietti, M., *Adv. Funct. Mater.*, **2007**, 17, 1010-1018
- <sup>8</sup> Demir-Cakan, R.; Baccile, N.; Antonietti, M.; Titirici, M.-M., *Chem. Mater.*, **2009**, 21, 484-490
- <sup>9</sup> Sun, X.; Li, Y. *Angew. Chem.*, **2004**, 116, 607-611
- <sup>10</sup> Zhao, L.; Baccile, N.; Gross, S.; Zhang, Y.; Wei W.; Sun, Y.; Antonietti, M.; Titirici, M.-M., *Carbon*, **2010**, 48, 3778-3787
- <sup>11</sup> Jia, Y. F.; Xiao, B.; Thomas, K. M., *Langmuir*, **2002**, 18, 470-478
- <sup>12</sup> Hulicova, D.; Kodama, M.; Hatori, H., *Chem. Mater.*, **2006**, 18, 2318-2326
- <sup>13</sup> Shao, Y. Y.; Sui, J. H.; Yin, G. P.; Gao, Y. Z. *Appl. Catal. B-Environ.*, **2008**, 79, 89-99
- <sup>14</sup> Plaza, M. G.; Pevida, C.; Arenillas, A.; Rubiera, F.; Pis, J. J., *Fuel*, **2007**, 86, 2204-12
- <sup>15</sup> Paraknowitsch, J. P.; Zhang, J.; Su, D.; Thomas, A.; Antonietti, M., *Adv. Mater.*, **2010**, 22, 87-92
- <sup>16</sup> Baccile, N.; Antonietti, M.; Titirici, M.-M., *ChemSusChem*, **2010**, 3, 246 - 253
- <sup>17</sup> Zhao, L.; Bacsik, Z.; Hedin, N.; Wei, W.; Sun, Y.; Antonietti, M.; Titirici, M.-M., *ChemSusChem*, **2010**, 3, 840-845
- <sup>18</sup> Zhao, L.; Fan, L.-Z.; Antonietti, M.; Titirici, M.-M., *Adv. Mater.*, **2010**, 22, 5202-5206
- <sup>19</sup> Fang, X.; Schmidt-Rohr, K., *J. Agric. Food Chem.*, **2009**, 57, 10701-10711
- <sup>20</sup> States, D. J.; Haberkorn, R. A.; Ruben, D. J., *J. Magn. Reson.*, **1982**, 48, 286
- <sup>21</sup> a) Cory, D. G.; Ritchey, W. M., *Macromolecules*, **1989**, 22, 1611 b) Alemany, L. B.; Grant, D. M.; Pugmire, R. J.; Alger, T. D.; Zilm, K. W., *J. Am. Chem. Soc.*, **1983**, 105, 2142

- 
- <sup>22</sup> a) Brinkmann, A.; Edén, M.; Levitt, M. H. J., **J. Chem. Phys.**, 2000, 112, 8539
- <sup>23</sup> a) Levy, G. C.; Lichter, R. L. Nitrogen-15 Nuclear Magnetic Resonance spectroscopy, Wiley, New York, 1979; b) Gammon, W. J.; Hoatson, G. L.; Holloway, B. C.; Vold, R. L.; Reilly, A. C., **Phys. Rev. B**, 2003, 68, 195401
- <sup>24</sup> a) Tressl, R.; Wondrak, G. T.; Garbe, L.-A.; Krueger, R.-P.; Rewicki, D., **J. Agric. Food Chem.**, 1998, 46, 1765-1776; b) Adams, A.; Tehrani, K. A.; Kersýiene, M.; Venskutonis, R.; De Kimpe, N., **J. Agric. Food Chem.**, 2003, 51, 4338-4343
- <sup>25</sup> a) Yaylayan, V. A.; Keyhani, A., **J. Agric. Food Chem.**, 2001, 49, 800-803, b) Haffenden, L. J. W.; Yaylayan, V. A., **J. Agric. Food Chem.**, 2005, 53, 9742-9746
- <sup>26</sup> Ames, J. M.; Bailey, R. G.; Mann, J., **J. Agric. Food Chem.**, 1999, 47, 438-443
- <sup>27</sup> Gandini, A.; Belgacem, M. N., **Prog. Polym. Sci.**, 1997, 22, 1203
- <sup>28</sup> Gandini, A.; Coelho, D.; Gome, M., **J. Mater. Chem.**, 2009, 19, 8656-8664